JOURNAL OF MATERIALS SCIENCE **40** (2005) 2213–2216

Surface tension of nickel, copper, iron and their binary alloys

J. BRILLO*, I. EGRY
Zentrum für Erstarrung unterkühlter Schmelzen ZEUS, Deutsches Zentrum für Luft- und Raumfahrt e.V., D-51170 Köln, Germany
E-mail: Juergen.Brillo@dlr.de

The surface tension of liquid binary alloys of the Cu-Ni-Fe system is measured by using the oscillating drop technique. The samples are processed contactlessly in an electromagnetic levitation chamber and hence, considerably large undercooling can be achieved. The alloys and the pure elements copper, nickel, and iron are investigated at various temperatures above and below their melting points. In addition, the surface tensions are also investigated as a function of the concentrations at constant temperature. The values agree well with predictions from theory and an analysis of the segregational behaviour is performed.

1. Introduction

From a thermodynamical point of view, the system Fe-Cu-Ni exhibits a variety of interesting features. It is known to possess a miscibility gap in the solid state for certain compositions only [1]. Furthermore, the binary systems Fe-Ni, Cu-Ni, and Cu-Fe display very different and partly opposite behaviours. While the energy of mixing ΔG is strongly negative for Fe-Ni, it is slightly positive for Cu-Ni and strongly positive for Fe-Cu. Also, Cu-Ni and Fe-Ni form a homogeneous solution at all temperatures and compositions, while this is not the case with Fe-Cu, where a miscibility gap exists in the undercooled region. Also, recently published density data [2] obtained for the liquid phase, yield excess volumes ΔV for each binary system. It was found that ΔV is nearly zero for Fe-Ni, negative for Cu-Ni and positive for Cu-Fe. The aim of this work is to measure the surface tensions of the binary systems in order to gather useful data and to obtain a more complete view of the system.

For a binary alloy, consisting of elements A and B, with corresponding surface tensions, $\sigma_{\mathrm{A}}(T)$ and $\sigma_{\mathrm{B}}(T)$, the surface tension is predicted by the Butler equation [3]:

$$\begin{aligned}\sigma_{\mathrm{AB}}(T) &= \sigma_{\mathrm{A}} + \frac{RT}{S_{\mathrm{A}}}\ln\left(\frac{1-c_{\mathrm{B}}^{\mathrm{S}}}{1-c_{\mathrm{B}}^{\mathrm{B}}}\right) + \frac{1}{S_{\mathrm{A}}} \\ &\quad\times\left\{\Delta G_{\mathrm{A}}^{\mathrm{S}}\left(T, c_{\mathrm{B}}^{\mathrm{S}}\right) - \Delta G_{\mathrm{A}}^{\mathrm{B}}\left(T, c_{\mathrm{B}}^{\mathrm{B}}\right)\right\} \\ &= \sigma_{\mathrm{B}} + \frac{RT}{S_{\mathrm{B}}}\ln\left(\frac{c_{\mathrm{B}}^{\mathrm{S}}}{c_{\mathrm{B}}^{\mathrm{B}}}\right) + \frac{1}{S_{\mathrm{B}}} \\ &\quad\times\left\{\Delta G_{\mathrm{B}}^{\mathrm{S}}\left(T, c_{\mathrm{B}}^{\mathrm{S}}\right) - \Delta G_{\mathrm{B}}^{\mathrm{B}}\left(T, c_{\mathrm{B}}^{\mathrm{B}}\right)\right\} \quad (1)\end{aligned}$$

where R: universal gas constant, T: temperature, S_{A}, S_{B}: surface areas in a monolayer of pure liquid A and B, $c_{\mathrm{A}}^{\mathrm{B}}$, $c_{\mathrm{B}}^{\mathrm{B}}$: mole fractions of A and B respectively in the bulk phase, and $c_{\mathrm{A}}^{\mathrm{S}}$, $c_{\mathrm{B}}^{\mathrm{S}}$: mole fractions of A, B in the surface phase. $\Delta G_{\mathrm{A}}^{\mathrm{B}}$, $\Delta G_{\mathrm{B}}^{\mathrm{B}}$ denote the partial excess Gibbs energy of A, B, in the bulk and $\Delta \mathrm{G}_{\mathrm{A}}^{S}$, $\Delta G_{\mathrm{B}}^{\mathrm{S}}$ are the partial excess Gibbs energy of A, B, in the surface layer. It was shown [4] that with sufficiently high accuracy, $\Delta G_{\mathrm{X}}^{\mathrm{S}}$ can be related to $\Delta G_{\mathrm{X}}^{\mathrm{B}}$ via

$$\Delta G_{\mathrm{X}}^{\mathrm{S}} \approx \frac{3}{4}\Delta G_{\mathrm{X}}^{\mathrm{B}} \quad (2)$$

with X being either A or B. The surface area S_{X} ($X = \mathrm{A,B}$) is calculated from the molar volume V_{X} as follows [4]: $S_{\mathrm{X}} = 1.091\ (6.02\ 10^{23})^{1/3} V_{\mathrm{X}}^{2/3}$ with V_{X} being the molar volume of component X.

2. Experimental

Experiments are carried out in a standard stainless steel vacuum chamber with a watercooled coil in its center. The coil is used for the electromagnetic levitation process. At the beginning of each experiment, the sample is located in the middle of the coil and the chamber is filled with 800 to 900 mbar of a gas mixture consisting of 92% He and 8% H_2, where hydrogen serves as a reducing agent. If a current of some 100 A at approximately 250 kHz is applied to the coil, electromagnetic forces lift the sample. At the same time, eddy currents inside the sample start heating and melting it. Cooling is performed by exposing the droplet to a laminar flow of the gas mixture which is admitted via a small ceramic tube at the bottom side of the sample. A detailed description of the levitation technique is given in [5].

For measuring the surface tension, a digital high speed camera (400 frames per sec, 1024 × 1000 pixels) is directed at the sample from the top. A series

*Author to whom all correspondence should be addressed.

of 4196 frames is recorded for each datapoint and is analysed afterwards by an edge detection algorithm. The algorithm applies the spatial derivative operator $||\mathrm{d}/\mathrm{d}x|| + ||\mathrm{d}/\mathrm{d}y||$ to the image and detects the edge of the sample. For the subsequent mathematical treatment, the edge points are expressed in polar coordinates with respect to the approximate drop center (x_0, y_0), so that they can be expressed as $R(\psi, t)$ with R being the radius, ψ ghe azimuthal angle and t the time at wich the frame was recorded. The radii for $\psi = 0$ and $\psi = \pi/2$ are of particular interest. Their frequency spectra exhibit a set of five peaks ω_m, $m = -2 \cdots 0 \cdots +2$, which belong to the $l = 2$ surface oscillation mode. The surface tension is calculated following the sum rule of Cummings and Blackburn [6]

$$\sigma = \frac{3M}{160\pi} \sum_{\mathrm{m}=-2}^{+2} \omega_\mathrm{m}^2 - 1.9\Omega^2 - 0.3\left(\frac{g}{a}\right)^2 \Omega^{-2} \quad (3)$$

with M being the mass of the sample, g the gravity constant and a the radius of the sample. Ω is calculated from the three translational frequencies ω_X, ω_Y, and ω_Z of the samples, e.g.:

$$\Omega^2 = \frac{1}{3}\left(\omega_\mathrm{X}^2 + \omega_\mathrm{Y}^2 + \omega_\mathrm{Z}^2\right) \quad (4)$$

A more detailed description of this procedure is given in references [6, 7].

The temperature of the sample is recorded by means of an infrared pyrometer that is directed to the sample also from the top, using a semitransparent mirror. For each sample, the liquidus temperature T_L was taken from reference [8]. The sample temperature T was obtained from calibrating the output signal T_P of the pyrometer by using the following approximation derived from Wien's law:

$$\frac{1}{T} - \frac{1}{T_\mathrm{P}} = \frac{1}{T_\mathrm{L}} - \frac{1}{T_\mathrm{L,P}} \quad (5)$$

In Equation 5, $T_\mathrm{L,P}$ is the pyrometer signal at the liquidus. Equation 5 is valid only if the emissivity $\varepsilon(T)$ remains constant over the experimentally scanned range of temperature. This is the case for most materials. However, in the case of iron-copper, extra care needs to be taken. In Fe-Cu, the emissivity is only constant when the temperature is above the binodal and when the melt is homogeneous. Furthermore, the surface tensions can only be measured at these temperatures, because equations 1,3 are not valid for a heterogeneous melt and need to be adapted, see reference [9].

3. Results and discussion

Fig. 1 presents the measured surface tension of Ni-Fe alloys versus temperature. The analysis of the data indicates that the surface tensions, σ, can be described as linear functions of temperature, T, also shown in Fig. 1:

$$\sigma(T) = \sigma_\mathrm{L} + \sigma_\mathrm{T}(T - T_\mathrm{L}) \quad (6)$$

In this equation, σ_L is the surface tension at the liquidus temperature, T_L, and σ_T is the thermal coefficient

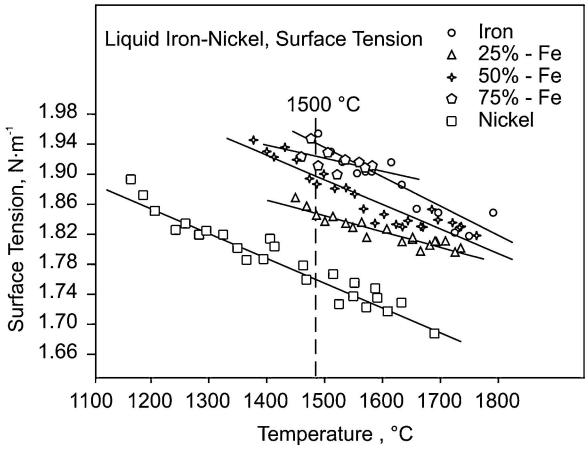

Figure 1 Surface tension data for levitated Fe-Ni alloys at different temperatures.

of the surface tension. The parameters σ_L, σ_T, and T_L are listed in Table I for each of the investigated samples respectively. Obviously, the magnitude of the surface tension increases with the increase of the iron content. From the fit parameters, σ_L and σ_T, the surface tension was calculated at $T = 1500°\mathrm{C}$ (marked by the dashed line in Fig. 1) for each concentration ion. The result is shown in Fig. 2. The same analysis was done for the two other systems, Cu-Ni and Cu-Fe, see Figs 3 and 4. In the case of Cu-Ni, the temperature chosen was 1272°C, and for Cu-Fe, it was 1550°C. In the three figures, the data are shown together with calculated data from Equation 1 with $\Delta G = 0$ and ΔG taken from refs. [4, 10, 11]. The parameters used to solve the Butler equation are listed in Tables II and III. The good agreement between the predicted values for $\Delta G \neq 0$ is obvious, but it is also obvious, that the ideal solution model ($\Delta G = 0$) does not apply in any of the cases. In Fig. 2, the strong increase of the surface tension with increasing iron content is somewhat surprising on the first sight, but it becomes plausible by the relative strong attractive interaction

TABLE I Fit parameters σ_L and σ_T of Equation 6 for each investigated material with corresponding liquidus temperature T_L

System	T_L (°C)	σ_L (N/m)	σ_T (10^{-4} N/m/K)
Cu	1084	1.29	−2.34
Fe	1538	1.92	−3.97
Ni	1454	1.77	−3.3
Ni75 Fe25	1440	1.73	−2.76
Ni50Fe50	1440	1.91	−3.27
Ni25Fe75	1473	1.93	−1.73
Cu10%Ni90%	1433	1.61	−0.67
Cu20%Ni80%	1417	1.51	−0.21
Cu30%Ni70%	1387	1.43	−0.84
Cu40%Ni60%	1347	1.38	−0.45
Cu50%Ni50%	1311	1.37	−0.94
Cu60%Ni40%	1280	1.36	−1.91
Cu70%Ni30%	1235	1.32	−3.24
Cu80%Ni20%	1189	1.34	−2.17
Cu90%Ni10%	1136	1.31	−2.21
Cu80 Fe20	1385	1.24	−3.84
Cu60 Fe40	1424	1.22	−4.4
Cu40Fe60	1435	1.24	−4.9
Cu20Fe80	1463	1.4	−6.42

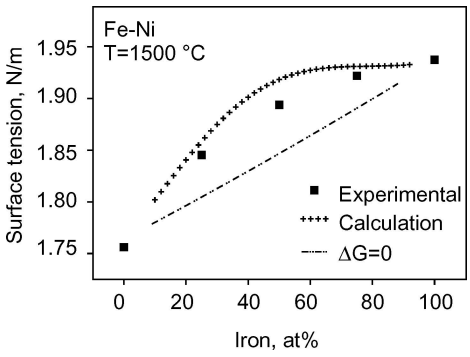

Figure 2 Surface tension, σ, of Fe-Ni at constant temperature $T = 1500°C$. The data are plotted as a function of the iron content in comparison with Equation 1 once for $\Delta G = 0$ (dash–dotted line) and ΔG taken from Table I (crosses).

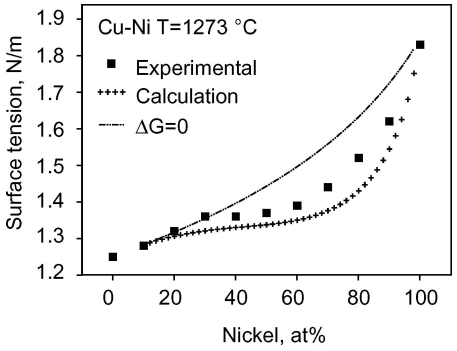

Figure 3 Surface tension, σ,of Cu-Ni at constant temperature $T = 1272°C$. The data are plotted as a function of the nickel content in comparison with equation (1) once for $\Delta G = 0$ (dash–dotted line) and ΔG taken from Table I (crosses).

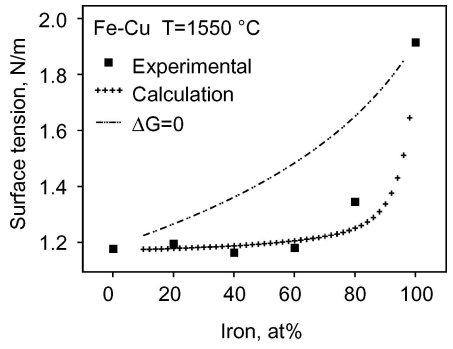

Figure 4 Surface tension, σ,of Cu-Fe at constant temperature $T = 1550°C$. The data are plotted as a function of the iron content in comparison with equation (1) once for $\Delta G = 0$ (dash-dotted line) and ΔG taken from Table I (crosses).

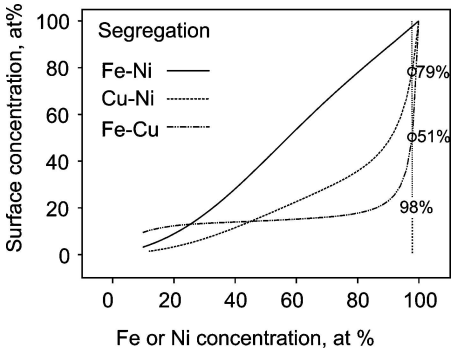

Figure 5 Surface concentration versus the bulk concentration for the three binary systems as calculated from Equation 1. The concentration is referred to nickel in the case of Fe-Ni and Cu-Ni and to iron in the case of Cu-Fe.

TABLE II Thermodynamic potentials ΔG used in Equation 1. For element X, the partial free enthalpy of mixing ΔG_X is related to the free enthalpy of of mixing ΔG according to $\Delta G_X = \Delta G + (1 - c_X)(\partial \Delta G / \partial c_X)$ [4]

System	Excess Gibbs energy ΔG, J/mole	Reference
Ni-Cu	$\Delta G = c_{Ni} \cdot c_{Cu}[(12048 + 1.29 \cdot T) + (-1861.6 + 0.942 \cdot T)(2c_{Ni} - 1)]$	[10]
Ni-Fe	$\Delta G = c_{Ni} \cdot c_{Fe}[(-8368 + 2.72 \cdot T)c_{Fe} + (-32217 + 9.205 \cdot T)c_{Ni}]$	[4]
Fe-Cu	$\Delta G = c_{Cu} \cdot c_{Fe}[(-36087.98 - 2.33 \cdot T) + (324.53 - 0.033 \cdot T)(2c_{Cu} - 1) + (10355.39 - 3.603 \cdot T)(2c_{Cu} - 1)^2]$	[11]

TABLE III Partial molar volumes V_X for element X, used to calculated the partial surface area $S_X$in Equation 1

Element	Partial molar volume V_X, 10^{-6} m^3 mol^{-1}	Reference
Ni	$7.43\ [1+1.51 \times 10^{-4}\ (T - T_L)°C^{-1}]$	[4]
Fe	$7.94\ [1+1.3 \times 10^{-4}\ (T - T_L)°C^{-1}]$	[4]
Cu	$7.43\ [1+1.0 \times 10^{-4}\ (T - T_L)°C^{-1}]$	[4]

between the iron and nickel atoms. The concentration in the surface region is also obtained from the Butler equation and is displayed in Fig. 5 for the three systems. For Fe-Ni, the concentration in the surface layer is almost the same as in the bulk, however the concentration of nickel on the surface is altered by a few percent compared to that in the bulk phase. In copper-nickel and copper-iron, copper becomes enriched in the surface region, due to its low surface tension and the positive ΔG, which is keeping the surface tension low for a broad range of nickel/iron concentration. For Cu-Ni the atomic concentration of nickel in the surface region is only 79% at 98% in the bulk. This ratio becomes even stronger in the case of Cu-Fe, where there is only 51% iron in the surface while 98% in the bulk. The latter might have some importance to the observation of the demixing in Cu-Fe. It has been argued, that while crossing the binodal and while demixing takes place, a sudden jump in the emissivity of the sample should be observable. According to Fig. 5, this however will not be the case as long as the iron concentration is lower than approximately 95%, because the outer shell of the sample consists of more than 80% of copper in the homogeneous solution already.

4. Summary

The surface tensions of the three binary alloy systems were measured. The data are reproduced by the Butler equation with ΔG taken from thermodynamic data bases. While Fe-Ni exhibits only a small deviation from the ideal segregation behaviour, this is not the case for Cu-Ni and Cu-Fe. Even at a high nickel or iron concentration of 98%, there is still a large amount of copper in the surface, which is 21% for Cu-Ni and 49% for Cu-Fe.

References

1. R. SCHMID, Y.-Y. CHUANG and Y. A. CHANG, *CALPHAD* **9** (1985) 383.

2. J. BRILLO and I. EGRY, *Z. Metallk.* **95** (2004) 691.
3. J. A. V. BUTLER, *Proc. Roy. Soc.* **135A** (1932) 348.
4. T. TANAKA and T. IIDA, *Steel Research* **65** (1994) 21.
5. D. M. HERLACH, R. F. COCHRANE, I. EGRY, H. J. FECHT and A. L. GREER, *Int. Mat. Rev.* **38** (1993) 273.
6. D. L. CUMMINGS and D. A. BLACKBURN, *J. Fluid Mech.* **224** (1991) 395.
7. S. SCHNEIDER, I. EGRY and I. SEYHAN, *Int. J. Thermophys.* **23** (2002) 1241.
8. T. B. MASSALSKI,"Binary Alloy Phase Diagrams" (American Society for Metals, 1986); I. Egry, *Z. Metallk.* **93** (2002) 528.
9. E. GORGES, Bestimmung der Dichte und Oberflächenspannung von levitierten flüssigen Metallegierungen am Beispiel des Systems Kupfer-Nickel, Ph.D. thesis, Rheinisch-Westfälische-Technische Hochschule, Aachen, 1996).
10. S. MEY, *Calphad* **16** (1992) 255.
11. SGTE Alloy Solution Database (Scientific Group Thermochemistry, Europe, 1992).

Received 31 March
and accepted 18 July 2004